Journal of Magnetism and Magnetic Materials 479 (2019) 84–87

Contents lists available at ScienceDirect

Journal of Magnetism and Magnetic Materials

journal homepage: www.elsevier.com/locate/jmmm

Research articles

Two modes of magnetic structure of nanocrystalline FeZrN films prepared by oblique-angle magnetron sputtering

E.N. Sheftel, E.V. Harin*

Baikov Institute of Metallurgy and Materials Science RAS, Leninsky pr. 49, Moscow 119334, Russia

ARTICLE INFO

Keywords:
Magnetic materials
Deposition
Correlation magnetometry
Random anisotropy model
Nanocrystalline materials
Thick films

ABSTRACT

The rf oblique-angle magnetron sputtering was used to prepare nanocrystalline $Fe_{77}Zr_7N_{16}$ (at.%) films (with grain size of 2–7 nm); the phase composition of the films is the α-Fe-based solid solution supersaturated with nitrogen and zirconium. The magnetic structure of the films is represented by stochastic domains. Using the correlation magnetometry method, two modes of stochastic domains were found, which correlate with two modes of the coercive force found in the magnetic hysteresis loops. Both modes of the coercive force are considered in terms of the random anisotropy model.

1. Introduction

Soft magnetic films are an important functional material used in the manufacture of modern and advanced microelectronics devices [1]. The basic requirements for such devices are miniaturization, performance and high sensitivity to weak magnetic fields.

Ferromagnetic nanocrystalline Fe-Me_{IV}X films (where Me_{IV} is IVA Group metals of the Periodic Table and X is nitrogen, carbon, or boron) produced by magnetron sputtering, the compositions of which are eutectic in metastable quasi-binary systems Fe-Me_{IV}X, are able to meet these requirements. This class of films ensures the unique combination of properties, namely, M_s up to 2 T [2], the coercive force less than 1 Oe [3,4], and the thermal stability up to 600 °C [2–4].

The high-frequency magnetic characteristics of ferromagnetic films applied in microelectronics devices are very important ones. One of the ways to obtain high magnetic permeability at high frequencies (MHz, GHz) is to increase the frequency of ferromagnetic resonance [5–7] by, in particular, creating the in-plane magnetic anisotropy [8–10]. As we know, the available literature data on the high-frequency magnetic properties of the Fe-Me_{IV}X nanocrystalline films are limited by single work [11].

In previously published work [3] the authors had studied nanocrystalline films of composition $Fe_{77}Zr_7N_{16}$ belonging to the above-mentioned class of Fe-Me_{IV}X films and prepared by oblique-angle magnetron sputtering, subjected to subsequent annealing. The correlation between static magnetic properties and phase composition as well material structure (grain size) was studied in [3].

The aim of the present work is study of the correlation between a coercive force and magnetic structure (local magnetic anisotropy in grain, macroscopic magnetic anisotropy in stochastic domain and domain size) of the same $Fe_{77}Zr_7N_{16}$ films.

2. Material and methods

The $Fe_{77}Zr_7N_{16}$ films 0.5 μm in thickness were prepared by rf reactive magnetron sputtering of a $Fe_{95}Zr_5$ target; the films were deposited on amorphous SiO_2 and multilayer $Si/SiO_2/Si_3N_4$ substrates, used in microelectronics, and which consist of single-crystal Si (with the 001 orientation), amorphous SiO_2 layer 0.4 μm thick, and Si_3N_4 layer (upper layer) 0.16 μm thick. The films were prepared by oblique-angle sputtering, i.e., the atomic flux makes an angle 0°, 10°, 20°, or 30°, with the normal to the substrate plane. Subsequent 1-h annealings were performed at 400 and 500 °C in a vacuum 10^{-6} mmHg. The specific composition of studied films and annealing conditions provide the best combination of saturation magnetization M_s and coercive force H_c [2–4]. The results of investigation of the structure by X-ray diffraction (XRD) analysis and induced magnetic anisotropy are available in detail in our previous study [3].

The chemical composition of the films was determined in a vacuum of 10^{-5} mmHg using a Quanta 200 scanning electron microscope equipped with an EDXRMA energy-dispersion X-ray attachment.

The nature of coercivity and magnetic permeability of nanocrystalline ferromagnets is considered in terms of the random anisotropy model [12]. When the grain size $2R_c$ is less than the exchange interaction length R_L, rms fluctuation of the local effective magnetic anisotropy field on the grain scale $D^{1/2}H_a$ is suppressed (D is the dispersion of

* Corresponding author.
E-mail address: harin-eugene@ya.ru (E.V. Harin).

https://doi.org/10.1016/j.jmmm.2019.02.027
Received 11 November 2018; Received in revised form 27 January 2019; Accepted 6 February 2019
Available online 06 February 2019
0304-8853/

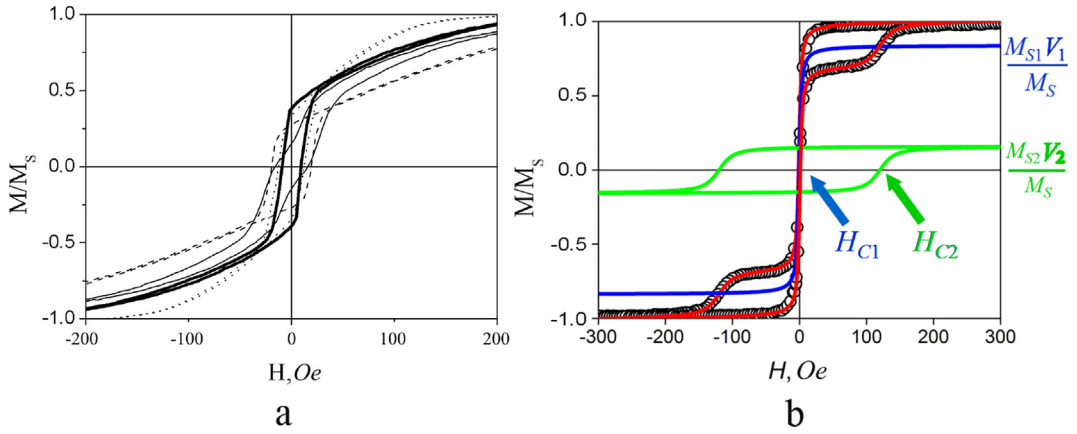

Fig. 1. Hysteresis loops of the $Fe_{77}Zr_7N_{16}$ film deposited on the $Si/SiO_2/Si_3N_4$ substrate: (a) as-sputtered at the deposition angle 0° (bold line), 10° (dashed line), 20° (dotted line), and 30° (thin line); (b) 20° annealed at 500 °C: experimental loop (open symbols) is fitted by sum of two loops (blue and green) characterized by relative magnetic moments $M_{s1}V_1/M_s$ and $M_{s2}V_2/M_s$, respectively.

magnetic anisotropy axes [12]). The magnetic hysteresis in low fields is determined by the macroscopic anisotropy field on the stochastic-domain scale $D^{1/2} < H_a >$, i.e., on the scale of uniform-magnetization area. This area, considered as a stochastic domain radius R_L, is an ensemble of N grains coupled with exchange interaction. Using the correlation magnetometry method [12] and the experimental magnetization curves measured at room temperature in fields up to 16 kOe, the parameters of local ($D^{1/2}H_a$) and macroscopic ($D^{1/2} < H_a >$) magnetic anisotropy fields and stochastic domain radius R_L were quantitatively estimated.

3. Results and discussion

According to XRD data [3], a nanocrystalline structure with grain size of 2–7 nm (depending on the deposition conditions) is formed in the films; the phase composition of the films is the α-Fe-based solid solution of nitrogen and zirconium.

The behavior of magnetic hysteresis loops measured for the studied films points to the existence of two magnetic anisotropies. This fact is indicated by a "step" in a field about 100 Oe (Fig. 1). To determine values of coercive forces (H_{c1} and H_{c2} in Fig. 1b) the hysteresis loops were approximated by the empirical Eq. (1) which can be considered as the modification of classical Langevin formula for magnetization process [13]. It follows from Eq. (1) that the experimentally determined magnetization (open symbols in Fig. 1b) is the algebraic sum of magnetization values corresponding to two hysteresis loops:

$$M(H) = M_{s1}V_1(cth(P_1(H \pm H_{c1})) - (P_1(H \pm H_{c1}))^{-1}) + M_{s2}V_2(cth(P_2(H \pm H_{c2})) - (P_2(H \pm H_{c2}))^{-1}) + \chi H, \quad (1)$$

where P_1, P_2, $M_{s1}V_1$, $M_{s2}V_2$ and χ are the adjustable parameters. If there are two phases in a film with different saturation magnetizations, they are summed in proportion to their volume fractions V_1 and V_2. Since it is impossible to define V_1 and V_2 in the framework of our approach we consider only the parameters $M_{s1}V_1$ and $M_{s2}V_2$.

The correlation magnetometry method [12] was used to quantitatively estimate parameters of local and macroscopic magnetic structures of the studied films. The existence of two coercive forces means the formation of stochastic domains characterized by the magnetic anisotropy fields, which differ in value, $D^{1/2} < H_a >_1$ and $D^{1/2} < H_a >_2$. Below they are shown as the 1st and 2nd modes of magnetic anisotropy field of stochastic domains, respectively.

To determine the parameters of the local and the macroscopic magnetic structures, the experimental magnetization curves of the films (Fig. 2a) were fitted by Eq. (2) in accordance with the method [12]:

$$M(H) = M_s(1 - (1/2)(D^{1/2}H_a)^2/(H^{1/2}H_R^{3/2} + H^2)), \quad (2)$$

where H is the external magnetic field; $D^{1/2}H_a$ is the local anisotropy field; M_s is the saturation magnetization; and H_R is the exchange field ($H_R = 2A/M_sR_c^2$, where A is the exchange stiffness and R_c is grain radius).

$D^{1/2}H_a$ values for all studied films are lower than the exchange field H_R (Table 1). According to [14], the exchange field is a threshold value of $D^{1/2}H_a$, below which ($D^{1/2}H_a < H_R$) the exchange interaction results in the stochastic domains formation. Thus, the magnetic structure formed in the studied films consists of stochastic domains.

Using estimated $D^{1/2}H_a$ and H_R values, the value of the 1st mode of anisotropy field of stochastic domains $D^{1/2} < H_a >_1$ and their size (Table 1) were determined by Eq. $D^{1/2} < H_a >_1 = (D^{1/2}H_a)^4/H_R^3$ and $2R_{L1} = 2R_c(H_R/D^{1/2}H_a)^2$, where $2R_c \approx 2 \div 7$ nm is grain size determined from XRD data [3].

It should be noted that the obtained inequality $2R_{L1} >> 2R_c$ (Table 1) for the studied films indicates the correctness of the consideration of their magnetic structure in terms of the random anisotropy model [14,15].

Correlation magnetometry method [14,16] provides an opportunity to determine the $D^{1/2}H_a$ and H_R parameters also by the graphical analysis of the magnetization dispersion $d_m = 1–M/M_s$ dependence on the external field H, which is plotted on log–log scale (Fig. 2b). Here, line I, described by Eq. (2), has two asymptotes: II is described by $d_m = (D^{1/2}H_a/H)^2$ (Akulov's law); III is described by $d_m = (D^{1/2}H_a)^2/(H_R^{3/2}H^2)$ (the decrease in the stochastic domain size with increasing field), from which the $D^{1/2}H_a$ and H_R values can be determined. Asymptote IV corresponding to a field range below few hundreds of oersteds is described by $d_m = (D^{1/2} < H_a >_2/H)^2$ [16]. Using the latter dependence, the 2nd mode of anisotropy field of stochastic domains $D^{1/2} < H_a >_2$ was determined. As is seen from Table 1, the $D^{1/2} < H_a >_2$ values exceed $D^{1/2} < H_a >_1$ by one or two orders of magnitude. When assuming that the field $D^{1/2} < H_a >_2$ is determined for an area with the characteristic size $2R_{L2} = 2R_c(H_R/D^{1/2} < H_a >_2)^{1/2}$, it follows that $2R_{L1} > 2R_{L2} > 2R_c$ (Table 1). It is assumed that the average effective parameters A, M_s, $2R_c$ and $D^{1/2}H_a$ remain unchanged over the entire film volume.

The appearance of two modes of magnetic anisotropy field of stochastic domains ($D^{1/2} < H_a >_1$ and $D^{1/2} < H_a >_2$) in nanocrystalline ferromagnet previously was noted in the literature; however, this phenomenon was related to the use of two different methods for estimating the same anisotropy field [14,16].

Although, we found that, as the deposition angle increases, the in-plane anisotropy field H_k increases and the lattice parameter of the α-Fe phase [3] decreases, however, it should be noted we failed to find the effect of the deposition angle on the magnetic structure parameters (Table 1). The absence of the effect of the deposition angle on the

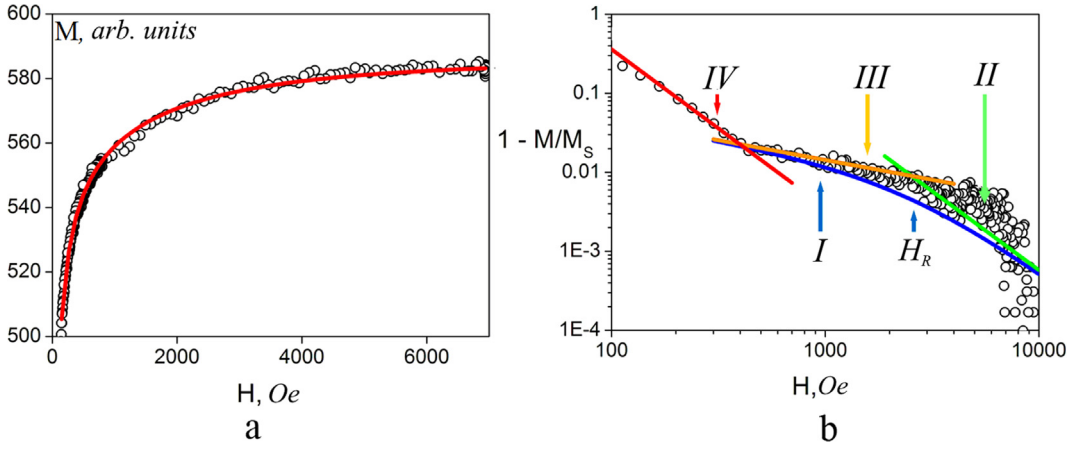

Fig. 2. Magnetization curves of the $Fe_{77}Zr_7N_{16}$ films in high magnetic fields: (a) magnetization curve for the film deposited on the SiO_2 substrate (deposition angle is 10°) and annealed at 500 °C, open symbols correspond to experimental data and solid line is fitting by Eq. (1); (b) field dependence of the magnetization dispersion $d_m = 1 - M/M_s$ plotted on log–log scale for the as-sputtered film deposited on the $Si/SiO_2/Si_3N_4$ substrate (deposition angle is 20°).

magnetic structure parameters can be explained by the fact that they were determined in sufficiently high magnetic fields (above 100 Oe, Fig. 2b, correlation magnetometry method), in which the induced magnetic anisotropy H_k (less than 40 Oe [3]) is suppressed by the external magnetic field.

It was found that $D^{1/2} < H_a >_1$ adequately correlates with the H_{c1} values (Fig. 3a). The decrease in the coercive force H_{c1} after annealing (the grain size almost is unchanged [3]) is resulted from changes of the magnetic structure described within the random anisotropy model [14,15]. The coercive force value H_{c2} (Fig. 1b) adequately correlates with $D^{1/2} < H_a >_2$ (Fig. 3a).

The values H_c and $D^{1/2} < H_a >$ can be affected by different factors, in particular, the magnetic anisotropy oriented perpendicular to the film surface. Such a magnetic anisotropy is formed in the studied as-sputtered films. This is indicated by the linear portion in the hysteresis loop of the films, which is observed in a field range above the H_c field (Fig. 1a).

Our previous electron-microscopic studies of these films [17] showed that during deposition and growth of the films the nano-sized grains form columnar-like aggregates growing perpendicular to the substrate surface. Such structure determines the formation of the perpendicular magnetic anisotropy in the as-sputtered films. As is seen from the magnetic hysteresis loops, the $D^{1/2} < H_a >_2$ values for the as-sputtered films correlate with the values of the perpendicular magnetic anisotropy field (Fig. 1a). It should be noted that the perpendicular magnetic anisotropy in as-sputtered films can be formed also by the negative magnetoelastic anisotropy caused by internal macrostresses [18].

The in-plane magnetic anisotropy can be related to the surface roughness [19,20], presence of nonferromagnetic inclusions [21], presence of two phases, which cannot be detected by XRD and are characterized by different saturation magnetizations [22], and also to positive magnetoelastic anisotropy [18].

In terms of the random anisotropy model when the coercive force is determined only by the exchange interaction between grains (the magnetization process is realized via the stochastic-domain magnetization rotation, $H_c = D^{1/2} < H_a >$), the value of coercive force is described by the expression $H_c \sim K_{eff}^4(2R_c)^6/(M_sA^3)$ [15]. For convenience, this relation can be transformed to the form $H_c/D^{1/2}H_a = (R_c/\delta)^6$, where $\delta = (A/K)^{1/2}$, $K = H_aM_s/2$ [16]. The R_c/δ ratio can be determined directly from results obtained by Eq. (2): $R_c/\delta = (R_L/R_c)^{-1/4}$. The dependence $H_c/D^{1/2}H_a = (R_c/\delta)^6$ was successfully checked by an example of nine different alloys [16].

For the studied films $Fe_{77}Zr_7N_{16}$, the correlation between $H_c/D^{1/2}H_a$ and R_c/δ in shown in Fig. 3b (solid line is $H_c/D^{1/2}H_a = (R_c/\delta)^6$, which is identical to $H_c = D^{1/2} < H_a >$). The found correlations both $H_{c1}/D^{1/2}H_a \sim R_c/\delta_1$ and $H_{c2}/D^{1/2}H_a \sim R_c/\delta_2$ mean that both coercive forces (H_{c1} and H_{c2}) satisfy the random anisotropy model, i.e., the both modes of the stochastic domain anisotropy field result from the exchange interaction between grains.

Taking into account the fact that the M_s, $D^{1/2}H_a$, and R_c magnitudes are identical for both stochastic domain modes, different magnitudes of

Table 1
Magnetic structure parameters of the studied $Fe_{77}Zr_7N_{16}$ films.

Deposition angle	Substrate	$D^{1/2} < H_a >_1$, Oe	$D^{1/2} < H_a >_2$, Oe	$D^{1/2}H_a$, Oe	H_R, Oe	$2R_{L1}$, nm	$2R_{L2}$, nm
As-sputtered films							
0°	$Si/SiO_2/Si_3N_4$	0.25 ± 0.15	60 ± 10	210 ± 20	1980 ± 340	210 ± 150	4.8 ± 0.9
10°		0.19 ± 0.13	100 ± 30	200 ± 25	2100 ± 440	340 ± 170	5.0 ± 1.2
20°		0.8 ± 0.5	85 ± 5	700 ± 90	6610 ± 1050	260 ± 100	10.2 ± 1.3
30°		0.6 ± 0.5	45 ± 20	1100 ± 210	13700 ± 3200	490 ± 280	22.3 ± 6
Annealed at 400 °C for 1 h							
0°	SiO_2	5.1 ± 2.6	11 ± 1	400 ± 30	1710 ± 220	94 ± 50	25.4 ± 3.2
10°		0.94 ± 0.9	70 ± 10	200 ± 15	1200 ± 150	110 ± 40	6.0 ± 0.8
20°		1.3 ± 0.9	7 ± 2	370 ± 60	2500 ± 540	92 ± 50	30.1 ± 7.8
30°		0.99 ± 0.5	30 ± 5	270 ± 13	1760 ± 120	170 ± 40	17.7 ± 2.6
Annealed at 500 °C for 1 h							
10°	SiO_2	11 ± 4	130 ± 20	860 ± 40	3600 ± 250	150 ± 40	20.2 ± 2.5
20°		5.8 ± 1.5	105 ± 15	490 ± 20	2150 ± 110	180 ± 30	19.7 ± 2.0
20°	$Si/SiO_2/Si_3N_4$	0.8 ± 0.7	90 ± 30	340 ± 100	2540 ± 990	1960 ± 1500	55.7 ± 19.3
30°		1.5 ± 0.4	90 ± 30	780 ± 580	6280 ± 5900	620 ± 580	50.3 ± 38.8

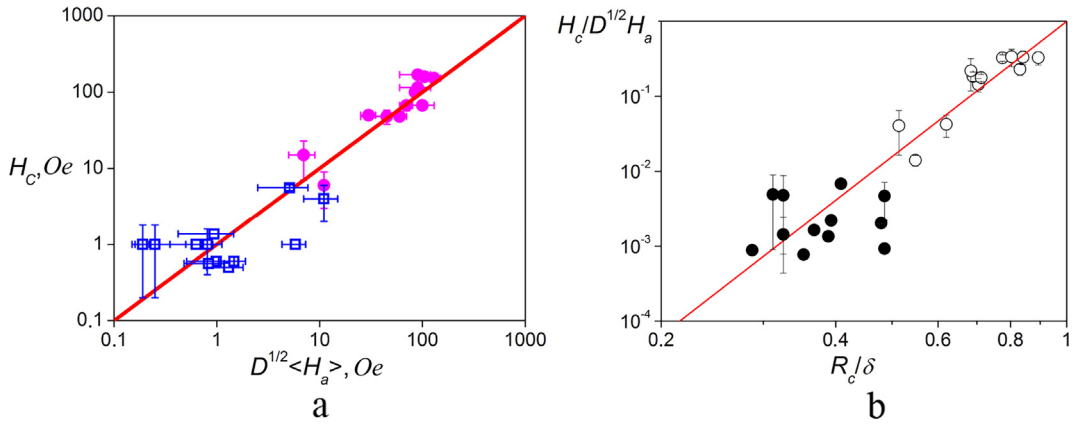

Fig. 3. (a) Correlation of two modes of magnetic anisotropy field ($D^{1/2} < H_a >_1$ and $D^{1/2} < H_a >_2$) and two coercive forces (H_{c1} and H_{c2}) for the studied films $Fe_{77}Zr_7N_{16}$: □ – $H_{c1} \sim D^{1/2} < H_a >_1$; ● – $H_{c2} \sim D^{1/2} < H_a >_2$. (b) Correlation of ratios $H_c/D^{1/2}H_a$ and R_c/δ: ● – $H_{c1}/D^{1/2}H_a \sim R_c/\delta_1$; ○ – $H_{c2}/D^{1/2}H_a \sim R_c/\delta_2$; solid line is $H_c/D^{1/2}H_a = (R_c/\delta)^6$.

exchange stiffness A (in $\delta = (A/K)^{1/2}$) are the cause for the formation of both domain modes. It should be noted that exchange stiffness inhomogenities in areas greater than the nano-sized grain were observed by spin-wave resonance technique [23]. The theoretical consideration of a similar structure is given in [24]. The results obtained by us, allow us to assume that a magnetic structure formed in the films is related to the presence of two ferromagnetic phases differing in the solid solution composition (and therefore in A values), which cannot be distinguished by XRD.

4. Conclusions

The rf oblique-angle magnetron sputtering was used to obtain nanocrystalline $Fe_{77}Zr_7N_{16}$ films (with grain size of 2–7 nm); the phase composition of the films is the α-Fe-based solid solution supersaturated with nitrogen and zirconium. The magnetic structure of the films, which is characterized by the existence of stochastic domains, is discussed in terms of the random anisotropy model. The correlation magnetometry method was used to determine the parameters of the magnetic structure: the local magnetic anisotropy field within a grain $D^{1/2}H_a$, the macroscopic magnetic anisotropy field within a stochastic domain volume $D^{1/2} < H_a >$, and stochastic domain radius R_L. It was found that two modes of the magnetic anisotropy field of stochastic domains $D^{1/2} < H_a >_1$ and $D^{1/2} < H_a >_2$ are formed, which differ in the exchange stiffness magnitude and determine the existence of two coercive forces.

The authors are grateful to Dr. N.B. Kolchugina for a useful discussion of the work.

Acknowledgements

This work was supported by the Russian Foundation for Basic Research (project no. 18-03-00502a).

References

[1] Sh. Fujii, K. Nishijima, H. Satoh, S. Yamamoto, J. Magn. Magn. Mater. 379 (2015) 256–259.
[2] E.N. Sheftel, E.V. Harin, Mat. Lett. 229 (2018) 36–39.
[3] E.N. Sheftel', E.V. Kharin, V.A. Tedzhetov, et al., Russ. Metall. 2016 (2016) 826–831.
[4] E.V. Harin, E.N. Sheftel', V.A. Tedzhetov, Tech. Phys. Lett. 44 (2018) 420–423.
[5] S.X. Wang, N.X. Sun, M. Yamaguchi, S. Yabukami, Nature 407 (6802) (2000) 150–151.
[6] M. Luo, P.H. Zhou, Y.F. Liu, et al., Mat. Lett. 188 (2017) 188–191.
[7] D. Li, Zh. Wang, X. Han, et al., J. Magn. Magn. Mat. 375 (2015) 33–37.
[8] X. Zhong, Ng. N. Phuoc, Y. Liu, C.K. Ong, J. Magn. Magn. Mat. 365 (2014) 8–13.
[9] P.N. Solovev, A.V. Izotov, B.A. Belyaev, J. Magn. Magn. Mat. 429 (2017) 45–51.
[10] X. Zhong, Ng.N. Phuoc, W.T. Soh, et al., J. Magn. Magn. Mat. 429 (2017) 52–59.
[11] N.G. Chechenin, C.B. Craus, A.R. Chezan, et al., IEEE Trans. Magn. 38 (2002) 3027–3029.
[12] S.V. Komogortsev, R.S. Iskhakov, J. Magn. Magn. Mat. 440 (2017) 213–216.
[13] I.E. Tamm, Fundamentals of the Theory of Electricity, Mir Publishers, Moscow, 1979.
[14] R.S. Iskhakov, S.V. Komogortsev, Phys. Met. Metallogr. 112 (2011) 666–681.
[15] G. Herzer, Acta Mater. 61 (2013) 718–734.
[16] R.S. Iskhakov, S.V. Komogortsev, Bull. Russ. Acad. Sci. Phys. 71 (2007) 1620–1622.
[17] O.M. Zhigalina, D.N. Khmelenin, E.N. Sheftel, et al., Crystallogr. Rep. 58 (2013) 344–354.
[18] A.R. Chezan, C.B. Craus, N.G. Chechenin, et al., J. Magn. Magn. Mat. 299 (2006) 219–224.
[19] E. Schlömann, J. Appl. Phys. 41 (1970) 1617–1622.
[20] C.-W. Cho, S.H. Park, J.S. Bae, S. Park, J. Magn. Magn. Mat. 354 (2014) 54–57.
[21] E.V. Harin, E.N. Sheftel, Phys. Met. Metallogr. 116 (2015) 753–759.
[22] S. Chikazumi, Physics of Ferromagnetism, second ed., Oxford University Press, London, 1997.
[23] B.P. Khrustalev, A.D. Balaev, V.G. Pozdnyakov, L.I. Vershinina, Solid State Commun. 55 (1985) 657–662.
[24] S. Komogortsev, S. Smirnov, R. Iskhakov, N. Momot, A. Balaev, L. Chekanova, E. Denisova, E. Eremin, Solid State Phenom. 168–169 (2011) 369–372.